Cancer Research

Genetic screening for synthetic lethal partners of polynucleotide kinase/phosphatase: potential for targeting SHP-1 depleted cancers

Todd R Mereniuk, Robert A Maranchuk, Anja Schindler, et al.

Cancer Res Published OnlineFirst September 7, 2012.

Genetic screening for synthetic lethal partners of polynucleotide kinase/phosphatase: potential for targeting SHP-1 depleted cancers

[1]Todd R. Mereniuk, [2]Robert A. Maranchuk, [2]Anja Schindler, [1]Jonathan Penner-Chea, [1]Gary K. Freschauf, [3]Samar Hegazy, [3]Raymond Lai, [2]Edan Foley, and [1]Michael Weinfeld

Affiliations of authors:
[1]Experimental Oncology, Department of Oncology, University of Alberta, Edmonton, AB, Canada T6G 1Z2
[2]Department of Medical Microbiology and Immunology, University of Alberta, Edmonton, AB, Canada T6G 2S2
[3]Department of Laboratory Medicine and Pathology, University of Alberta, Edmonton, AB, Canada T6G 1Z2

Correspondence to: Michael Weinfeld
Cross Cancer Institute
University of Alberta
11560 University Ave
Edmonton, AB, Canada, T6G 1Z2
Tel: 780 432 8438
Fax: 780 432 8428
E-mail: michael.weinfeld@albertahealthservices.ca.

Running title: Synthetic lethal partnership between PNKP and SHP-1

Word count: 6225

Total number of Figures in main text - 7
Total number of Tables in main text - 0
Total number of Figures in Supplementary material - 7
Total number Tables in Supplementary material – 2

Key words: Synthetic lethality, genetic screen, reactive oxygen species, polynucleotide kinase/phosphatase, SHP-1

Conflict of Interest: Todd Mereniuk, Edan Foley and Michael Weinfeld have submitted a Provisional US patent application - UNAB 017 Synthetic lethality in cancer.

ABSTRACT

A genetic screen using a library of 6961 siRNAs led to the identification of SHP1 (PTPN6), a tumor suppressor frequently mutated in malignant lymphomas, leukemias and prostate cancer, as a potential synthetic lethal partner of the DNA repair protein polynucleotide kinase/phosphatase (PNKP). After confirming the partnership with SHP-1, we observed that co-depletion of PNKP and SHP-1 induced apoptosis. A T-cell lymphoma cell line that is SHP-1-deficient (Karpas 299) was shown to be sensitive to a chemical inhibitor of PNKP, but resistance was restored by expression of wild-type SHP-1 in these cells. We determined that while SHP-1 depletion does not significantly impact DNA strand-break repair, it does amplify the level of reactive oxygen species (ROS) and elevate endogenous DNA damage. The ROS scavenger WR1065 afforded protection to SHP-1 depleted cells treated with the PNKP inhibitor. We propose that co-disruption of SHP-1 and PNKP leads to an increase in DNA damage that escapes repair, resulting in the accumulation of cytotoxic double-strand breaks and induction of apoptosis. This supports an alternative paradigm for synthetic lethal partnerships that could be exploited therapeutically.

INTRODUCTION

A recent exciting development in cancer treatment is the potential utilization of synthetic lethality as a patient and cancer-specific therapy. Synthetic lethality arises when the simultaneous disruption of two non-allelic, non-essential genes or their proteins in the same cell induces lethality (1, 2). Recently this phenomenon has been shown to occur between combinations of DNA repair genes and much attention has focused on the co-disruption of the single-strand break repair (SSBR) protein poly(ADP-ribose) polymerase (PARP) and the breast cancer associated (BRCA) proteins (3-5), which are naturally lost or mutated in tumor cells of women afflicted with hereditary breast and ovarian cancer and have roles in DNA double-strand break repair (DSBR). One proposed explanation for this synthetic lethality is that chemical inhibition of PARP causes the generation of double-strand breaks (DSBs) by preventing SSBR (6, 7). As cells progress through S-phase, naturally occurring SSBs collapse the replication fork to give rise to DSBs, which in $BRCA^{-/-}$ cancer cells accumulate, eventually leading to cancer cell death. Normal cells in BRCA patients retain BRCA heterozygosity and therefore possess the capacity to fully repair DSBs and so are not appreciably affected by PARP inhibitors during the treatment, and thus the deleterious side effects typically associated with cancer therapy are greatly reduced (8).

It has been estimated that there are approximately 10^4 SSBs formed per cell per day probably as a result of the generation of reactive oxygen species (ROS) during normal metabolism (9). Many of these breaks harbour unligatable termini such as 3'-phosphates and 5'-hydroxyls that must be processed for DNA repair to proceed. Polynucleotide kinase/phosphatase (PNKP) is a bifunctional enzyme whose role is to

process these termini during SSBR and DSBR by catalyzing the dephosphorylation of 3'-phosphate termini and the phosphorylation of 5'-hydroxyl termini to yield elongation and ligation-competent 5'-phosphate and 3'-hydroxyl ends (10). PNKP is a versatile protein acting in many DNA repair pathways, including base excision repair (BER), SSBR and DSBR (10). Cells stably depleted of PNKP show marked sensitization to γ-radiation and the topoisomerase I inhibitor camptothecin (11).

Given the potential to target PNKP by small molecule inhibitors (12), we sought to identify synthetic lethal relationships of PNKP in order to expand the repertoire of targeted therapy taking advantage of this approach. By screening ~7000 genes targeting the "druggable" genome, we have identified a variety of proteins potentially synthetic lethal with PNKP including several that are either known or are implicated as tumor suppressors, such as the protein tyrosine phosphatase SHP-1 (PTPN6). We also show that SHP-1 is likely not directly involved in DNA repair and therefore cell death based on DSB accumulation caused by inhibition of two distinct but interacting DNA repair pathways, i.e. SSBR and DSBR as previously described, is not the only explanation for the occurrence of synthetic lethality involving a DNA repair protein partner (6, 7). Instead, the observation that SHP-1 depletion causes an increase in ROS production supports an alternative paradigm for synthetic lethality that combines increased DNA damage production with limited DNA repair capacity, as was previously shown for the interaction between PTEN-induced putative kinase 1 (PINK1) and the mismatch repair proteins MSH2, MLH1 and MSH6 (13). This suggests that we can broaden the potential for clinical application of synthetic lethality.

MATERIALS AND METHODS

Cells

A549 (human lung carcinoma) and MCF7 (human breast adenocarcinoma) cell lines were obtained from the American Type Culture Collection (Manassas, VA), who performed short tandem repeat profiling of each cell line before shipment. The cells were cultured for 2-3 weeks to generate stocks that were then kept frozen until used for the current experiments. These cells and their transfected derivatives were cultured at 37°C and 5% CO_2 in a humidified incubator in a 1:1 mixture of Dulbecco's Modified Eagle's Medium and F12 (DMEM/F12) supplemented with 10% fetal bovine serum (FBS), L-glutamine (2 mM), non-essential amino acids (0.1 mM) and sodium pyruvate (1 mM). All culture supplements were purchased from Invitrogen (Carlsbad, CA). For comet assays and apoptosis/necrosis detection penicillin (50 U/mL) and streptomycin (50 μg/mL) were added to the DMEM/F12 (complete DMEM/F12). SUPM2 (DCMZ, Braunschweig, Germany) and Karpas 299 (obtained as a gift from Dr. M. Kadin, Boston, MA) human anaplastic large cell lymphoma cell lines were cultured in RPMI-1640 medium (Sigma-Aldrich, Oakville, ON) supplemented with 10% FBS, 0.3 g/L L-glutamine and 2 g/L $NaHCO_3$. Both SUPM2 and Karpas 299 cells were recently confirmed to carry monoclonal T-cell rearrangements by polymerase chain reaction and express the NPM-ALK fusion protein by western blots.

Stable transfection

All cell lines were generated by stable transfection of pSUPER.neo constructs (Oligoengine, Seattle, WA) into A549 or MCF7 cells yielding several distinct cell lines.

An shRNA directed against nucleotides 1391-1410 of PNKP (11) was used to stably deplete PNKP in A549 and MCF7 cells (A549δPNKP and MCF7δPNKP, respectively), and another shRNA expression vector targeting nucleotides 1313-1333 of SHP-1 was used to generate A549δSHP-1 cells. A control cell line was also generated in which an shRNA to no known gene target (a scrambled shRNA, pSUPER.neo.Mamm-X, Oligoengine) was expressed in A549 cells (A549-Scramble).

Approximately 20,000 A549 or MCF7 cells were plated and allowed to adhere overnight in a 24-well dish at 37°C and 5% CO_2. Lipofectamine2000 (Invitrogen) was used according to the manufacturer's instructions to transfect cells with the shRNA plasmid constructs. The cells were then trypsinized and replated into 6 x 100-mm plates in DMEM/F12 without antibiotics and incubated overnight at 37°C and 5% CO_2. The following day, media was removed and replaced with complete DMEM/F12 containing 500 μg/mL G418. After single-clone colonies were formed (10-18 days) the colonies were picked and expanded prior to protein analysis.

Transient transfections

Approximately 4,000 A549δPNKP, A549-Scramble, MCF7δPNKP or MCF7 cells were plated per well in a 96-well plate, and allowed 24 h to adhere in a humidified incubator at 37°C and 5% CO_2. All wells surrounding samples were filled with 100 μL distilled water to control for evaporation effects. For protocol optimization and initial verification of selected hits, 56 nM final concentration of siRNA was added to 50 μL total reaction volume in Opti-MEM (Invitrogen). At the same time as siRNA-Opti-MEM incubation, a 1:25 dilution of Dharmafect Transfection Reagent 1 (Dharmacon, Lafayette,

CO) in Opti-MEM was allowed to incubate at room temperature for 5 min, to provide a final volume of 0.23 μL transfection reagent per well. The two transfection solutions were then combined and held at room temperature for 20 min. The media was then removed from the cells and 100 μL of the transfection mixture was added per well and the plate was incubated at 37°C and 5% CO_2 for 72 h. All siRNAs were purchased from Qiagen (Mississauga, ON).

Protein analysis

Western blots were conducted using 50 μg of whole cell lysate. Monoclonal antibody towards PNKP (H101) was used as previously described (14) and was incubated at 1:1000 in 5% PBSMT (PBS with 5% w/v skim milk and 0.1% Tween-20) overnight at 4°C. Polyclonal primary antibodies (SHP-1 and β-actin) were incubated (1:4000 dilution) in 5% PBSMT for 1 h at room temperature (Santa Cruz Biotechnology, Santa Cruz, CA). All secondary antibodies were incubated (1:5000 dilution) for 45 min at room temperature (Jackson ImmunoResearch Laboratories, Inc. West Grove, PA).

siRNA library screen

Qiagen's "Druggable" genome siRNA library is comprised of four sub-classifications: phosphatases, kinases, G-protein coupled receptors and uncategorized proteins consisting of 205, 696, 490 and 5570 mRNA targets, respectively. The library was first distributed into 89 x 96-well plates at a total siRNA concentration of 1 μM, each well containing a pool of four separate siRNAs to the same mRNA target. Also added to the plates were three additional control wells (C12, D12 and E12) of AllStars Negative

(ASN) scrambled siRNA (Qiagen). Then, utilizing a JANUS Automated Workstation (PerkinElmer, Waltham, MA), 4,000 A549δPNKP or A549-Scramble cells were seeded into each well of a 96-well plate in a final volume of 100 μL DMEM/F12 without penicillin/streptomycin and allowed to adhere overnight in a humidified incubator. The following day, transfection mixture was generated as described above (56nM siRNA and a total of 0.23 μL Dharmafect transfection reagent 1 per well), media was aspirated from the wells, and 100 μL of the mixture was added to each well and allowed to incubate for 72 h. Then 10% v/v of 440 μM Alamar Blue (Sigma-Aldrich, Oakville, ON) was added to each well and the cells were incubated for 50-90 min, after which the fluorescence in each well was determined using an EnVision 2104 Multilabel Reader (PerkinElmer) with an excitation wavelength of 563 nm and emission wavelength of 587 nm (15). Each screen was performed in duplicate. A result was deemed a potential synthetic lethal hit if survival under the simultaneous knockdown condition was ≤33% when compared to the internal plate controls average.

Transient transfections of siRNAs for synthetic lethal partners were used for confirmatory assays, however each siRNA was used independently and at a concentration of 20 nM. All other reagent concentrations remained constant. Each assay was performed manually and the fluorescence was read with a FLUOstar Optima® plate reader (BMG Labtec Inc. Durham, NC) using excitation and emission wavelengths of 563 and 587 nm, respectively.

Statistical analysis

R^2 values were generated in Microsoft Excel by plotting individual survival scores

from the duplicate screen against one another. All p-values were generated using a two-sided Student's t-test. Z-scores were only generated for confirmatory data where an average from 23-96 individual wells of data per assay (performed at least in triplicate) were measured, allowing us an appropriate number of replicates to achieve robust statistical data. A Z-score is a dimensionless quantity representing a measurement of the number of standard deviations a sample is above or below the mean of a control. It is defined as:

$$z = \frac{x - \mu}{\sigma}$$

z = Z-score
x = the raw score to be standardized
μ= population mean
σ = standard deviation of the population

As such, Z-scores can be positive or negative depending on whether the sample is higher or lower than the mean of a control. For our results, we were interested in a negative Z-score as this showed that the survival of the experimental condition was lower than control (i.e. the condition was lethal). A sample with a Z-score of -3 or less is significantly different than control and is a threshold often used in synthetic lethal screens.

Cell proliferation assay with anaplastic large cell lymphoma (ALCL) cell lines

Karpas 299, SUPM2 or Karpas 299 (SHP-1-complemented) cells were plated in 96-well format at a density of 5,000 cells/100 µL in complete RPMI. Increasing concentrations of the PNKP inhibitor A12B4C3 was added to each well in a constant volume of DMSO and left to incubate for 12-16 days. Eleven µL of 440 µM Alamar Blue was then added to each well and left to incubate for 24-48 h after which fluorescence was

determined as described above. At least 3 independent experiments were performed with either 48 or 96 replicates for each experiment.

A pCI expression vector (Promega, Madison, WI) was used to transiently re-express SHP-1 in Karpas 299 cells (16). The Karpas 299 cells were grown in antibiotic-free RPMI after which 10^7 cells were harvested per transfection in 500 μL total volume of antibiotic-free RPMI. These cells were placed into a 4-mm electroporation cuvette (VWR, Radnor, PA) together with 10 μg of plasmid DNA. The cells were then electroporated using a BTX ECM 300 square electroporator (BTX Technologies Inc., Holliston, MA) at 225 V for three pulses of 8.5 ms. The cells were then transferred to 20 mL of antibiotic-free RPMI and incubated for 24 h before experimentation.

Determination of mode of cell death

A549-Scramble or A549δPNKP cells were grown on coverslips in complete DMEM/F12 and transfected with either ASN or SHP-1 siRNA. As a positive control for apoptosis the cell lines were treated with 100 μM 5-(p-bromobenzylidine)-α-isopropyl-4-oxo-2-thioxo-3-thiozolidineacetic acid (BH3I-1, Sigma-Aldrich, Oakville, ON), which is a potent apoptosis inducer. The cells were grown under each condition for the indicated length of time before being subjected to a triple stain of Hoechst 33342, Ethidium Homodimer III and Annexin V-FITC as described by the kit manufacturer (Biotium, Hayward, CA). Each experiment was performed in duplicate, with ten random microscope fields chosen per duplicate. The data were combined to generate a higher total number of cells counted. Between 250-1000 cells for each time point were counted.

Detection of γH2AX

To monitor the level of H2AX phosphorylation before and after γ-radiation, 1 x 10^5 cells (A549-Scramble or A549δSHP-1) were seeded on coverslips in 35-mm dishes with 2 mL DMEM/F12 without antibiotics and left overnight to adhere in a humidified incubator. The cells were then irradiated (5 Gy) and left to repair for the indicated time points, after which γH2AX was measured as previously described (17). Fluorescence was normalized to background fluorescence and quantified using ImageJ (http://rsbweb.nih.gov/ij/). For accumulation of DSBs under PNKP inhibition in the absence of irradiation, 5 μM A12B4C3 (or 100 μM BH3I-1 as control for apoptosis-induced H2AX phosphorylation) was added to the media at the time of plating, and left for 48 h. Fluorescence quantification was then performed as described above.

Detection of reactive oxygen species (ROS)

The presence of hydroxyl radicals and peroxynitrite was detected using a commercial kit (Cell Technology, Mountain View, CA). Cells were grown in 96-well format and transfected with either ASN or SHP-1 siRNA for 24 h prior to ROS detection. Cells were rinsed twice with modified Hanks balanced salt solution (HBSS) supplemented with 10 mM HEPES, 1 mM $MgCl_2$, 2 mM $CaCl_2$ and 2.7 mM glucose, after which 100 μL of aminophenyl fluorescein (APF) or hydroxyphenyl fluorescein (HPF), diluted to 10 μM in the same modified HBSS, was applied to the cells for 45 min at 37°C in the dark. The plates were then read using a FLUOstar Optima® plate reader at an excitation wavelength of 488 nm and an emission wavelength of 515 nm.

Colony-forming assay

A549δSHP-1 and A549-Scramble cells were plated in the presence of increasing concentrations of A12B4C3 alone, or with or without the ROS scavenger WR1065. Cells were subjected to these conditions continuously for 10-14 days after which plates were stained with crystal violet and counted (11). Colonies containing fewer than 30 cells were omitted.

RESULTS

siRNA screen for the synthetic lethal partners of PNKP

We sought to discover synthetic lethal partnerships of PNKP, as an alternative to PARP, without necessarily limiting our search to partner proteins directly involved in DNA repair. We performed an unbiased forward transfection screen using an extensive library of siRNAs targeting 6961 genes, in which a pool of four distinct siRNAs targets each gene. Two duplicate screens were performed; the first utilized A549 lung cancer cells stably depleted of PNKP (A549δPNKP), and the second A549 cells expressing a scrambled shRNA (A549-Scramble) under identical conditions. (The level of PNKP in the knockdown and control cells is shown in Supplemental Fig. 1A). Cells were exposed to siRNA continuously for 72 h (allowing for at least two cell cycles to occur) at a concentration known to be effective at knocking down target proteins (data not shown). Cell survival was then determined by an Alamar Blue-based fluorescence assay (15).

Cell survival scores after targeting each of the 6961 mRNAs were compared to an average internal plate control located on every plate screened, consisting of the average survival of 3 wells of the cells screened (A549δPNKP or A549-Scramble) transiently

transfected with Allstars negative scrambled control siRNA (ASN) under identical screen conditions. Genes and their corresponding proteins were classified as potential hits for synthetic lethality with PNKP if the survival under the simultaneous knockdown condition was ≤33% when compared to the internal plate controls average. A comparison of the duplicate screens showed that an overwhelming majority of the siRNAs yielded reproducible phenotypes (Supplemental Fig. 2) and a summary of the data derived from the mean values is outlined in Figure 1. Most of the proteins identified as potential 'hits' in the screen were lethal only in combination with PNKP disruption and were not singularly lethal (for comparison SHP-1 data is graphically represented alongside two randomly selected proteins deemed "non-hits", Supplemental Fig. 3).

A master list of potential synthetic lethal partners is shown in Supplemental Table 1. The positive hit rate was found to be 6.1% (425/6961) including 8 phosphatases, 97 kinases, 117 G-protein coupled receptors and 203 unclassified proteins. Of note, 14 tumor suppressors were identified as potentially synthetically lethal with PNKP (Supplemental Table 2).

Confirmation of SHP-1 as a possible synthetic lethal partner of PNKP

One potential hit for synthetic lethality with PNKP identified in the screen was SHP-1, a protein tyrosine phosphatase that has been implicated as a tumor suppressor, functioning in the regulation of signal transduction pathways (18) to counter growth-promoting and oncogenic signals through its phosphatase activity (19). To confirm the synthetic lethal relationship between PNKP and SHP-1, we repeated the analysis, but reduced the concentration of siRNA previously used in the screen from 56 to 20 nM and

used each of the four originally pooled siRNAs separately in order to minimize the potential for off-target effects and limit toxicity in A549-Scramble cells transfected with the SHP-1 siRNA. When the distinct SHP-1 siRNAs were assayed, all four displayed selective killing of A549δPNKP cells and no or limited toxicity in control cells (Fig. 2A, siRNA#5 Z-factor = -12.3, $p < 0.001$; siRNA#10 Z-factor = -17.2, $p < 0.001$, siRNA#11 Z-factor = -6.88, $p < 0.001$, siRNA#6 Z-factor = -6.44, $p < 0.001$). Since all four siRNAs showed synthetic lethality with PNKP, as well as the capacity to deplete SHP-1 protein (Supplemental Fig. 1B), the effect was most likely attributable to the simultaneous depletion of PNKP and SHP-1, and not due to off-target effects. Furthermore, the lack of toxicity seen using ASN control siRNA with A549δPNKP cells indicated that non-specific activation of the RNAi pathway was not responsible for the observed lethality.

To further substantiate that a synthetic lethal partnership exists between SHP-1 and PNKP, we carried out a similar analysis with the MCF7 breast cancer cell line. We performed the cell proliferation assay using 20 nM of SHP-1 siRNA#5 with an MCF7 cell line stably depleted of PNKP (MCF7δPNKP). As seen with A549 cells, the combined disruption of both SHP-1 and PNKP was responsible for lethality, since the depletion of PNKP or SHP-1 individually was not lethal (Fig. 2B, Z-score = -3.4, $p < 0.001$), nor was the activation of RNAi machinery alone responsible for lethality (Fig. 2B). Similarly, in the reciprocal experiment, in which stable SHP-1 depleted A549 cells (A549δSHP-1) or A549-Scramble cells were transfected with siRNA targeting PNKP (Fig. 2C) or exposed to a small molecule inhibitor of PNKP 3'-phosphatase activity, A12B4C3 (12), lethality was only observed when both PNKP and SHP-1 were disrupted (Fig. 2D).

We also show that small molecule inhibition or siRNA-mediated knockdown of PARP1 is insufficient to cause a lethal effect in A549δSHP-1 cells (Supplemental Fig. 4), indicating that PARP1 cannot substitute for PNKP in synthetic lethal relationships with SHP-1, and therefore for some tumors PNKP may serve as an alternative therapeutic target to PARP1.

Mode of cell death

To identify the mechanism by which cells undergo disrupted SHP-1/PNKP-mediated synthetic lethality, A549-Scramble and A549δPNKP cells were grown on coverslips and transiently transfected with ASN or SHP-1 siRNA. As a positive control, cells were treated with the apoptosis inducer BH3I-1. Cells were then simultaneously stained with Hoechst 33342, Ethidium Homodimer III and Annexin V-FITC. Hoechst 33342 stains the nuclei of healthy and unhealthy cells alike, while Ethidium Homodimer III identifies cells that are in late stage of apoptosis or are necrotic, and Annexin V identifies early apoptotic cells. Figure3A shows there was a small population of apoptotic and necrotic cells following transfection of both cell lines with ASN. As expected, treatment with BH3I-1 induced a substantial increase in apoptosis in both cell lines (Fig. 3B). Co-disruption of SHP-1 and PNKP by transient transfection of SHP-1 siRNA into the PNKP-depleted cell line also caused a substantial increase in the proportion of apoptotic cells, with only a small increase in the necrotic population (Fig. 3C). In contrast, no induction of apoptosis was observed following transient transfection of SHP-1 siRNA in the cell line expressing scramble shRNA. Thus these data indicate that cells undergoing SHP-1/PNKP induced synthetic lethality do so by an apoptotic mechanism.

Survival of naturally occurring SHP-1 positive and negative cells in response to PNKP inhibition

The utility of synthetic lethality will lie in the capacity to translate potential associations into targeted therapy, possibly using inhibitors of one of the partners as a single agent. To investigate the feasibility of taking advantage of the newly identified partnership between SHP-1 and PNKP, we subjected two anaplastic large cell lymphoma cell lines, Karpas 299 (naturally SHP-1 deficient) and SUPM2 (which expresses SHP-1), to an increasing concentration of the PNKP inhibitor, A12B4C3, over a period of 12-16 days. The dose response curves (Fig. 4) indicate that at A12B4C3 doses $\geq$ 10 μM there was a marked decrease in survival of the Karpas 299 cells, while the SUPM2 cells remained viable. To confirm the central role of SHP-1 in the observed response we expressed wild-type SHP-1 in Karpas 299 cells (western blot shown in Supplemental Fig. 1C), and these cells displayed reduced sensitivity to A12B4C3.

Underlying mechanism of the PNKP/SHP-1 synthetic lethal partnership

The mechanism for synthetic lethality involving PARP1 and BRCA1 or 2 is considered to be an interplay between two DNA repair pathways (3, 4, 7, 20), and thus to date, there has been considerable focus on the critical involvement of both proteins of a synthetic lethal partnership in DNA surveillance or repair (6, 8, 20-25). SHP-1 is a protein tyrosine phosphatase known to negatively regulate receptor tyrosine kinase signaling (18, 26). There is no evidence to date to indicate that SHP-1 is involved in DNA repair. We therefore sought to determine if SHP-1 plays a major role in regulating

DSB or SSB repair. Accordingly, A549-Scramble and A549δSHP-1 cells were irradiated and DSBR was followed by visualizing the formation of γH2AX foci as well as by single-cell gel electrophoresis (comet assay) under neutral conditions and SSBR by comet assay under alkaline conditions. A549-Scramble and A549δSHP-1 cells showed reasonably similar kinetics (Fig. 5) for the formation and removal of γH2AX foci over the course of 24 h following irradiation, suggesting that loss of SHP-1 did not significantly affect the rate of repair of DSB, although a greater number of foci appeared to be generated in the first 15 minutes following irradiation of A549δSHP-1 cells. Interestingly, there was also a notable presence of γH2AX foci in the unirradiated A549δSHP-1 cells and a proportionately higher level of foci at each time point after irradiation, including the 24 h time point when almost all foci had disappeared in the A549-Scramble cells. The results of the γH2AX assay were supported by the neutral comet assay (Supplemental Figs. 5 and 6). DSBR in irradiated A549-Scramble cells was almost complete by 24 h (Supplemental Fig. 6A). In contrast, the loss of a recognized DNA repair enzyme such as PNKP (A549δPNKP cells) severely retarded the rate of repair (Supplemental Fig. 6B), in agreement with previous observations (27). The A549δSHP-1 cells showed a similar rate of DSBR as A549-Scramble cells (Supplemental Fig. 6C), again indicating that SHP-1 does not play a significant role in DSBR, but there was a noticeably elevated level of DSB present in the untreated A549δSHP-1 cells as evidenced by a large proportion of cells showing type 2 comets or above (Supplemental Fig. 6C).

When A549-Scramble cells were subjected to the alkaline comet assay (Supplemental Fig. 6), we observed total repair of radiation-induced SSBs after 120 minutes (Supplemental Fig. 6D) in marked contrast to DNA repair deficient A549δPNKP

cells (Supplemental Fig. 6E). SHP-1 knockdown cells showed a very similar response to radiation as A549-Scramble cells, indicating that SHP-1 is not significantly involved in the repair of SSBs (Supplemental Fig. 6F), but, as with the DSB data, we observed a modestly higher level of SSBs in the unirradiated SHP-1 depleted cells than in the controls.

The results above render it unlikely that the primary cause of the synthetic lethal partnership between PNKP and SHP-1 is due to an interaction between two DNA repair pathways akin to PARP and the BRCA proteins, and we therefore sought an alternative explanation. One clue provided by the repair assays was the higher level of strand breaks in the unirradiated SHP-1 depleted cells, which, together with reports in the literature regarding elevated levels of ROS in SHP-1 depleted cells (28), led us to an alternative hypothesis that reduced SHP-1 expression leads to the generation of ROS-induced DNA strand-breaks, the repair of which are dependent on PNKP activity. To investigate this supposition, we examined the basal level of ROS (hydroxyl radicals and peroxynitrite together) produced in the wild-type and SHP-1 depleted cells that were used to establish the synthetic lethal partnership between PNKP and SHP-1. We found that when SHP-1 was depleted to approximately 15% of wild-type level, ~40% more ROS were produced in both A549 and MCF7-based cell lines (Figs. 6A and B).

To further corroborate a role for ROS in the synthetic lethal partnership between PNKP and SHP-1, we treated A549-Scramble and A549δSHP-1 cells with the PNKP inhibitor, A12B4C3, in the presence or absence of the ROS scavenger WR1065 (29, 30) to determine if a reduction in cellular ROS concentration would rescue the lethal phenotype conferred to cells upon co-disruption of PNKP and SHP-1 (Fig. 6C). (Doses of

the two chemical reagents were chosen so as to avoid toxicity in the control A549-Scramble cells). In the absence of the ROS scavenger, treatment of the A549δSHP-1 cells with A12B4C3 resulted in ~30% cytotoxicity, which contrasts with the almost complete abrogation of cytotoxicity when A12B4C3 was co-administered with WR1065, implicating a critical role for ROS in the PNKP/SHP-1 synthetic lethal partnership.

Finally an examination of the influence of PNKP inhibition on the ROS-induced DSBs, in which A549δSHP-1 and A549-Scramble cells were treated with a non-toxic dose of A12B4C3 and the level of H2AX phosphorylation was monitored over 48 hours, revealed that DSBs accumulate when SHP-1 and PNKP are simultaneously depleted (Fig.7).

DISCUSSION

Synthetic lethality is a promising avenue for cancer therapy and even in its early development appears to be clinically effective (31, 32). Our screen identified 425 possible synthetic lethal partners of PNKP, representing 6.1% of genes tested, which is typical for initial screens of this type (33-35). Of these proteins, 14 are currently considered to be tumor suppressors, including PTEN and SHP-1. From the standpoint of potential therapeutic benefit in cancer treatment there is clearly considerable advantage to identifying partnerships of tumor suppressors. The participation of some tumor suppressors in synthetic lethal partnerships has been noted before. PTEN has a partnership with PARP (22), which has been attributed to reduced DSBR by homologous recombination (36), while p53 has been shown to have synthetic lethal partnerships with the protein kinases SGK2 and PAK3 (37). Loss-of-function mutants are considered

notoriously hard to treat, as protein function is difficult to re-establish pharmacologically and re-establishment of tumor suppressor activity is technically challenging. However, through the use of the concept of synthetic lethality, such mutant cells become targetable (38, 39). This is possible because in principle synthetic lethality targets the tumor suppressor's lethal partner, thereby only affecting the naturally protein deficient cancer cells to cause the cytotoxic double disruption, effectively leaving normal cells unharmed. Side effects are therefore theorized to be minor, and in practice this can be seen. In the clinical trials using Olaparib in BRCA1- and BRCA2-mutated ovarian cancer, the only grade 3 toxicities observed were nausea (7%) and leukopenia (5%) (40).

Of the tumor suppressors identified, we chose to further validate SHP-1 as it has been shown to be deficient or absent in a substantial number of human cancers (18, 26, 41). Tissue microarray analysis of the SHP-1 status of 207 paraffin-embedded samples of a diverse assortment of malignant lymphomas and leukemias revealed that ≥90% of diffuse large cell lymphoma, follicle center lymphoma, Hodgkin's disease, mantle cell lymphoma, peripheral T cell lymphoma, adult T cell lymphoma/leukemia specimens and 100% of NK/T cell lymphoma specimens showed no detectable SHP-1 expression (41-43). Similarly, SHP-1 was expressed at reduced or undetectable levels in 40 of 45 malignant prostate samples (42). This raises the possibility that clinically effective inhibitors of PNKP or other synthetic lethal partners of SHP-1 may provide substantial benefit to patients with these particular cancers.

The mode of synthetic lethality-induced cell death is of clinical interest. Cells undergoing necrosis lose membrane integrity early and release cytotoxic constituents that can damage neighboring cells, or induce an undesirable immune response (44). However,

apoptotic cells do not cause such an immune response. They are recognized by the host immune system and phagocytized by macrophages in a highly regulated process required for tissue homeostasis and immune regulation (44). Therefore, apoptosis may be an advantageous mode of cell death for cells undergoing synthetic lethality (44-46).

As the number of newly discovered synthetic lethal partnerships increases, it will be important to define their respective underlying biochemical mechanisms. To date, most attention has focused on partnerships between enzymes involved in DNA single- and double-strand break repair pathways. In our examination of DSBR (Fig. 5), we observed a greater production of γH2AX foci over the first 15 min post-irradiation in the A549δSHP-1 cells than in the A549-Scramble cells. This could be interpreted as slower repair of DSB, but alternatively it could reflect a higher level of free radicals as discussed below. It is noticeable that, similar to the control cells, there was a marked decline in foci in theA549δSHP-1 cells by the 4-hour time point, indicative of efficient DSBR. This data coupled with our observation of efficient SSBR (Supplemental Fig. 6) led us to look for an alternative mechanism for SHP-1/PNKP synthetic lethality. It has been observed previously that SHP-1 depletion causes an increase in ROS production in HUVEC cells through its negative regulation of NAD(P)H-oxidase–dependent superoxide production (28). Furthermore, SHP-1, in common with many other protein-tyrosine phosphatases, is susceptible to oxidation of key cysteine residues in its catalytic domain by reactive oxygen species, including those generated by ionizing radiation (47, 48). Our data (Fig. 6) indicate that SHP-1 depletion in A549 and MCF7 cells also causes an increase in ROS production, which in turn results in elevated DNA strand cleavage (Fig. 5 and Supplemental Fig. 6). (Radiation-induced inactivation of the residual SHP-1 present in

the SHP-1 knockdown cells, and the resulting increase in ROS, could explain the higher production of γH2AX foci in these cells at 15 min post-irradiation). We inferred that, when coupled with PNKP-mediated disruption of DNA repair, increased ROS production causes a cytotoxic accumulation of DNA damage (Fig. 7). The elimination of cytotoxicity conferred by treatment with the free radical scavenger WR1065 (Fig. 6C) provided additional support for such a mechanism. Since PNKP acts on SSBs, as well as DSBs, an increase in unrepaired ROS-induced SSBs would lead to an increase in DSB formation during S-phase, potentially saturating DSB repair because these newly-formed DSBs would also require the action of PNKP at their termini. Our findings further extend the observation by Martin et al. (13), who showed that depletion of PINK1 causes an elevation of ROS and toxicity in a mismatch-repair deficient background. Importantly, this mechanism may apply to other yet to be identified synthetic lethal partnerships between proteins involved in ROS regulation and oxidative DNA damage repair.

ACKNOWLEDGEMENTS

We thank Dr. Aghdass Rasouli-Nia for technical support and Dr. Sunita Ghosh for statistical support. Dr. Robert Ingham (Department of Medical Microbiology and Immunology, University of Alberta) for assistance with electroporation of Karpas cells.

FINANCIAL SUPPORT

This work was supported by the Canadian Institutes of Health Research (grant numbers MOP 15385 and MOP 115069 to MW; MOP 77746 to EF). TRM is the recipient of graduate studentships from the Alberta Cancer Foundation and Alberta Innovates -

Health Solutions. EF is a scholar of Alberta Innovates – Health Solutions and holds a Canada Research Chair in Innate Immunity.

REFERENCES

1. Lucchesi JC. Synthetic lethality and semi-lethality among functionally related mutants of Drosophila melanogaster. Genetics. 1968;59:37-44.
2. Iglehart JD, Silver DP. Synthetic lethality--a new direction in cancer-drug development. N Engl J Med. 2009;361:189-91.
3. Bryant HE, Schultz N, Thomas HD, Parker KM, Flower D, Lopez E, et al. Specific killing of BRCA2-deficient tumours with inhibitors of poly(ADP-ribose) polymerase. Nature. 2005;434:913-7.
4. Farmer H, McCabe N, Lord CJ, Tutt AN, Johnson DA, Richardson TB, et al. Targeting the DNA repair defect in BRCA mutant cells as a therapeutic strategy. Nature. 2005;434:917-21.
5. Fong PC, Boss DS, Yap TA, Tutt A, Wu P, Mergui-Roelvink M, et al. Inhibition of poly(ADP-ribose) polymerase in tumors from BRCA mutation carriers. N Engl J Med. 2009;361:123-34.
6. Bolderson E, Richard DJ, Zhou BB, Khanna KK. Recent advances in cancer therapy targeting proteins involved in DNA double-strand break repair. Clin Cancer Res. 2009;15:6314-20.
7. Helleday T. The underlying mechanism for the PARP and BRCA synthetic lethality: Clearing up the misunderstandings. Mol Oncol. 2011;5:387-93.
8. Amir E, Seruga B, Serrano R, Ocana A. Targeting DNA repair in breast cancer: a clinical and translational update. Cancer Treat Rev. 2010;36:557-65.
9. Lindahl T, Nyberg B. Rate of depurination of native deoxyribonucleic acid. Biochemistry. 1972;11:3610-8.
10. Weinfeld M, Mani RS, Abdou I, Aceytuno RD, Glover JN. Tidying up loose ends: the role of polynucleotide kinase/phosphatase in DNA strand break repair. Trends Biochem Sci. 2011;36:262-71
11. Rasouli-Nia A, Karimi-Busheri F, Weinfeld M. Stable down-regulation of human polynucleotide kinase enhances spontaneous mutation frequency and sensitizes cells to genotoxic agents. Proc Natl Acad Sci U S A. 2004;101:6905-10.
12. Freschauf GK, Karimi-Busheri F, Ulaczyk-Lesanko A, Mereniuk TR, Ahrens A, Koshy JM, et al. Identification of a small molecule inhibitor of the human DNA repair enzyme polynucleotide kinase/phosphatase. Cancer Res. 2009;69:7739-46.
13. Martin SA, Hewish M, Sims D, Lord CJ, Ashworth A. Parallel high-throughput RNA interference screens identify PINK1 as a potential therapeutic target for the treatment of DNA mismatch repair-deficient cancers. Cancer Res. 2011;71:1836-48.
14. Fanta M, Zhang H, Bernstein N, Glover M, Karimi-Busheri F, Weinfeld M. Production, characterization, and epitope mapping of monoclonal antibodies against human polydeoxyribonucleotide kinase. Hybridoma. 2001;20:237-42.
15. Schindler A, Foley E. A functional RNAi screen identifies hexokinase 1 as a modifier of type II apoptosis. Cell Signal. 2010;22:1330-40.
16. Hegazy SA, Wang P, Anand M, Ingham RJ, Gelebart P, Lai R. The tyrosine 343 residue of nucleophosmin (NPM)-anaplastic lymphoma kinase (ALK) is important for its

interaction with SHP1, a cytoplasmic tyrosine phosphatase with tumor suppressor functions. J Biol Chem. 2010;285:19813-20.
17. Ismail IH, Andrin C, McDonald D, Hendzel MJ. BMI1-mediated histone ubiquitylation promotes DNA double-strand break repair. J Cell Biol. 2010;191:45-60.
18. Irandoust M, van den Berg TK, Kaspers GJ, Cloos J. Role of tyrosine phosphatase inhibitors in cancer treatment with emphasis on SH2 domain-containing tyrosine phosphatases (SHPs). Anticancer Agents Med Chem. 2009;9:212-20.
19. Wu C, Sun M, Liu L, Zhou GW. The function of the protein tyrosine phosphatase SHP-1 in cancer. Gene. 2003;306:1-12.
20. Dedes KJ, Wilkerson PM, Wetterskog D, Weigelt B, Ashworth A, Reis-Filho JS. Synthetic lethality of PARP inhibition in cancers lacking BRCA1 and BRCA2 mutations. Cell Cycle. 2011;10:1192-9.
21. Stefansson OA, Jonasson JG, Johannsson OT, Olafsdottir K, Steinarsdottir M, Valgeirsdottir S, et al. Genomic profiling of breast tumours in relation to BRCA abnormalities and phenotypes. Breast Cancer Res. 2009;11:R47.
22. Mendes-Pereira AM, Martin SA, Brough R, McCarthy A, Taylor JR, Kim JS, et al. Synthetic lethal targeting of PTEN mutant cells with PARP inhibitors. EMBO Mol Med. 2009;1:315-22.
23. Gien LT, Mackay HJ. The Emerging Role of PARP Inhibitors in the Treatment of Epithelial Ovarian Cancer. J Oncol. 2010;2010:151750.
24. Chan N, Bristow RG. "Contextual" synthetic lethality and/or loss of heterozygosity: tumor hypoxia and modification of DNA repair. Clin Cancer Res. 2010;16:4553-60.
25. Martin SA, McCabe N, Mullarkey M, Cummins R, Burgess DJ, Nakabeppu Y, et al. DNA polymerases as potential therapeutic targets for cancers deficient in the DNA mismatch repair proteins MSH2 or MLH1. Cancer Cell. 2010;17:235-48.
26. Kharitonenkov A, Chen Z, Sures I, Wang H, Schilling J, Ullrich A. A family of proteins that inhibit signalling through tyrosine kinase receptors. Nature. 1997;386:181-6.
27. Freschauf GK, Mani RS, Mereniuk TR, Fanta M, Virgen CA, Dianov GL, et al. Mechanism of action of an imidopiperidine inhibitor of human polynucleotide kinase/phosphatase. J Biol Chem. 2010;285:2351-60.
28. Krotz F, Engelbrecht B, Buerkle MA, Bassermann F, Bridell H, Gloe T, et al. The tyrosine phosphatase, SHP-1, is a negative regulator of endothelial superoxide formation. J Am Coll Cardiol. 2005;45:1700-6.
29. Dziegielewski J, Baulch JE, Goetz W, Coleman MC, Spitz DR, Murley JS, et al. WR-1065, the active metabolite of amifostine, mitigates radiation-induced delayed genomic instability. Free Radic Biol Med. 2008;45:1674-81.
30. Walker DM, Kajon AE, Torres SM, Carter MM, McCash CL, Swenberg JA, et al. WR1065 mitigates AZT-ddI-induced mutagenesis and inhibits viral replication. Environ Mol Mutagen. 2009;50:460-72.
31. Audeh MW, Carmichael J, Penson RT, Friedlander M, Powell B, Bell-McGuinn KM, et al. Oral poly(ADP-ribose) polymerase inhibitor olaparib in patients with BRCA1 or BRCA2 mutations and recurrent ovarian cancer: a proof-of-concept trial. Lancet. 2010;376:245-51.
32. Glendenning J, Tutt A. PARP inhibitors--current status and the walk towards early breast cancer. Breast.20 Suppl 3:S12-9.

33. Colombi M, Molle KD, Benjamin D, Rattenbacher-Kiser K, Schaefer C, Betz C, et al. Genome-wide shRNA screen reveals increased mitochondrial dependence upon mTORC2 addiction. Oncogene. 2011;30:1551-65.
34. Naik S, Dothager RS, Marasa J, Lewis CL, Piwnica-Worms D. Vascular Endothelial Growth Factor Receptor-1 Is Synthetic Lethal to Aberrant {beta}-Catenin Activation in Colon Cancer. Clin Cancer Res. 2009;15:7529-37.
35. Azorsa DO, Gonzales IM, Basu GD, Choudhary A, Arora S, Bisanz KM, et al. Synthetic lethal RNAi screening identifies sensitizing targets for gemcitabine therapy in pancreatic cancer. J Transl Med. 2009;7:43.
36. McEllin B, Camacho CV, Mukherjee B, Hahm B, Tomimatsu N, Bachoo RM, et al. PTEN loss compromises homologous recombination repair in astrocytes: implications for glioblastoma therapy with temozolomide or poly(ADP-ribose) polymerase inhibitors. Cancer Res. 2010;70:5457-64.
37. Baldwin A, Grueneberg DA, Hellner K, Sawyer J, Grace M, Li W, et al. Kinase requirements in human cells: V. Synthetic lethal interactions between p53 and the protein kinases SGK2 and PAK3. Proc Natl Acad Sci U S A. 2010;107:12463-8.
38. Canaani D. Methodological approaches in application of synthetic lethality screening towards anticancer therapy. Br J Cancer. 2009;100:1213-8.
39. Chan DA, Giaccia AJ. Harnessing synthetic lethal interactions in anticancer drug discovery. Nat Rev Drug Discov. 2011;10:351-64.
40. Underhill C, Toulmonde M, Bonnefoi H. A review of PARP inhibitors: from bench to bedside. Ann Oncol. 2010.
41. Oka T, Yoshino T, Hayashi K, Ohara N, Nakanishi T, Yamaai Y, et al. Reduction of hematopoietic cell-specific tyrosine phosphatase SHP-1 gene expression in natural killer cell lymphoma and various types of lymphomas/leukemias : combination analysis with cDNA expression array and tissue microarray. Am J Pathol. 2001;159:1495-505.
42. Cariaga-Martinez AE, Lorenzati MA, Riera MA, Cubilla MA, De La Rossa A, Giorgio EM, et al. Tumoral prostate shows different expression pattern of somatostatin receptor 2 (SSTR2) and phosphotyrosine phosphatase SHP-1 (PTPN6) according to tumor progression. Adv Urol. 2009:723831.
43. Delibrias CC, Floettmann JE, Rowe M, Fearon DT. Downregulated expression of SHP-1 in Burkitt lymphomas and germinal center B lymphocytes. J Exp Med. 1997;186:1575-83.
44. Krysko DV, D'Herde K, Vandenabeele P. Clearance of apoptotic and necrotic cells and its immunological consequences. Apoptosis. 2006;11:1709-26.
45. Baehrecke EH. How death shapes life during development. Nat Rev Mol Cell Biol. 2002;3:779-87.
46. deBakker CD, Haney LB, Kinchen JM, Grimsley C, Lu M, Klingele D, et al. Phagocytosis of apoptotic cells is regulated by a UNC-73/TRIO-MIG-2/RhoG signaling module and armadillo repeats of CED-12/ELMO. Curr Biol. 2004;14:2208-16.
47. Heneberg P, Draber P. Regulation of cys-based protein tyrosine phosphatases via reactive oxygen and nitrogen species in mast cells and basophils. Curr Med Chem. 2005;12:1859-71.
48. Barrett DM, Black SM, Todor H, Schmidt-Ullrich RK, Dawson KS, Mikkelsen RB. Inhibition of protein-tyrosine phosphatases by mild oxidative stresses is dependent on S-nitrosylation. J Biol Chem. 2005;280:14453-61.

FIGURE LEGENDS

Figure 1. Overall survey of the screens for synthetic lethality with PNKP. The screens were performed using a forward transfection protocol with A549 cells stably depleted of PNKP (A549δPNKP) and cells stably expressing a scrambled siRNA (A549-Scramble). The first bar on the left represents the total mean cell survival values generated by the siRNAs targeting proteins deemed as potential synthetic lethal hits with PNKP designated on the basis of survival of an arbitrary cutoff of ≤33% compared to internal plate controls, which were normalized to 100% and represented by the bar on the far right. The second bar from the left represents the cell survival of the entire screen using A549δPNKP cells including the potential hits. The third bar from the left shows the mean survival of the A549-Scramble cells treated with the siRNAs identified as potential hits in the A549δPNKP screen. The difference between the first and third bars imply that most of the siRNAs causing lethality in A549δPNKP cells do not do so in the control A549-Scramble cells and thus require PNKP depletion to induce cytotoxicity.

Figure 2. Confirmation of synthetic lethality between SHP-1 and PNKP. (A) Four distinct siRNAs (20 nM) targeting SHP-1 expression were used to transiently transfect both A549δPNKP and A549-Scramble cell lines. Error bars represent standard error (± S.E.) from at least three independent determinations. All SHP-1 siRNAs were lethal only when combined with PNKP disruption. Transient transfection with a control (Allstars negative, ASN) siRNA failed to elicit a cytotoxic response indicating that activation of the RNAi machinery was not responsible for cell killing. (B) Confirmation of the SHP-1/PNKP synthetic lethal relationship using MCF7 and MCF7δPNKP (MCF7 cells stably depleted

of PNKP) cells. (C) Survival of A549δSHP-1 and A549-Scramble cells transiently transfected with an siRNA against PNKP. (D) Survival of A549δSHP-1 cells exposed to increasing concentration of the PNKP phosphatase inhibitor A12B4C3. Error bars represent standard error (± S.E.) from at least three independent determinations.

Figure 3. Mode of cell death of cells undergoing synthetic lethality due to the simultaneous disruption of SHP-1 and PNKP. (A) A549δPNKP and A549-Scramble cells were transiently transfected with ASN control siRNA and apoptosis and necrosis was determined over a 72-hour period as described in Materials and Methods at times after transfection. (B) Additional treatment of the ASN-transfected cells with the potent apoptosis inducer BH3I-1. (C) Induction of apoptosis and necrosis in A549δPNKP and A549-Scramble cells transiently transfected with SHP-1 siRNA.

Figure 4. Survival of anaplastic large cell lymphoma cells under PNKP inhibition. Karpas 299 (naturally lacking functional SHP-1), SUP-M2 cells (which express normal levels of SHP-1), Karpas 299 cells expressing SHP-1 (Karpas 299+SHP-1) and vector only controls (Karpas 299+pCI) were treated with increasing concentrations of the PNKP inhibitor A12B4C3 for 12-16 days. Survival was measured using an Alamar Blue-based fluorescence assay. Error bars represent standard error (± S.E.) from at least three independent determinations.

Figure 5. Influence of SHP-1 on double-strand break repair. Cells were subjected to γ-radiation (5 Gy) and the repair of DSBs was monitored by H2AX phosphorylation. (A)

Typical staining of unirradiated and irradiated A549-Scramble and A549δSHP-1 cells, showing staining with nuclear stain DAPI (left-hand column) and γH2AX antibody (middle column), and overlay (right-hand column). (B) Quantification of the average integrated fluorescence intensity per nucleus due to phosphorylation of histone H2AX as a function of time after 5-Gy irradiation. Error bars represent ± standard error of the mean. (The level of SHP-1 depletion in A549δSHP-1 cells is shown in Supplemental Fig. 1D).

Figure 6. Depletion of SHP-1 causes an increase in production of ROS. (A) Expression of SHP-1 was transiently knocked down using siRNA in A549-based cell lines and production of ROS was measured as described in Materials and Methods. The cell lines are listed on top and the siRNA used is listed in parentheses below. Error bars represent standard deviation (± S.D.) from at least three independent determinations carried out in duplicate. (B) Data obtained with MCF7-based cell lines under identical conditions. (C) Rescue of lethal phenotype upon addition of ROS scavenger WR1065. A549δSHP-1 cells were subjected to 1 or 5 μM A12B4C3 in the presence or absence of 10 μM of the ROS scavenger WR1065 in a colony-forming assay. A549-Scramble cells treated with 10 μM WR1065 showed no toxicity at the concentrations tested. All marked values are statistically significant at $p < 0.01$. Error bars represent standard error (± S.E.) from at least three independent determinations.

Figure 7. Inhibition of PNKP in A549δSHP-1 cells causes an accumulation of DSBs. (A) A549-Scramble and A549δSHP-1 cells were subjected to 5 μM A12B4C3 and

phosphorylation of H2AX was monitored. (B) Quantification of the average integrated fluorescence intensity per nucleus due to phosphorylation of histone H2AX as a function of time after addition of A12B4C3. As a control for the potential induction of γH2AX foci by apoptosis we treated the A549-Scramble cells with BH3I-1 (Supplemental Fig. 7). Error bars represent ± standard error of the mean.

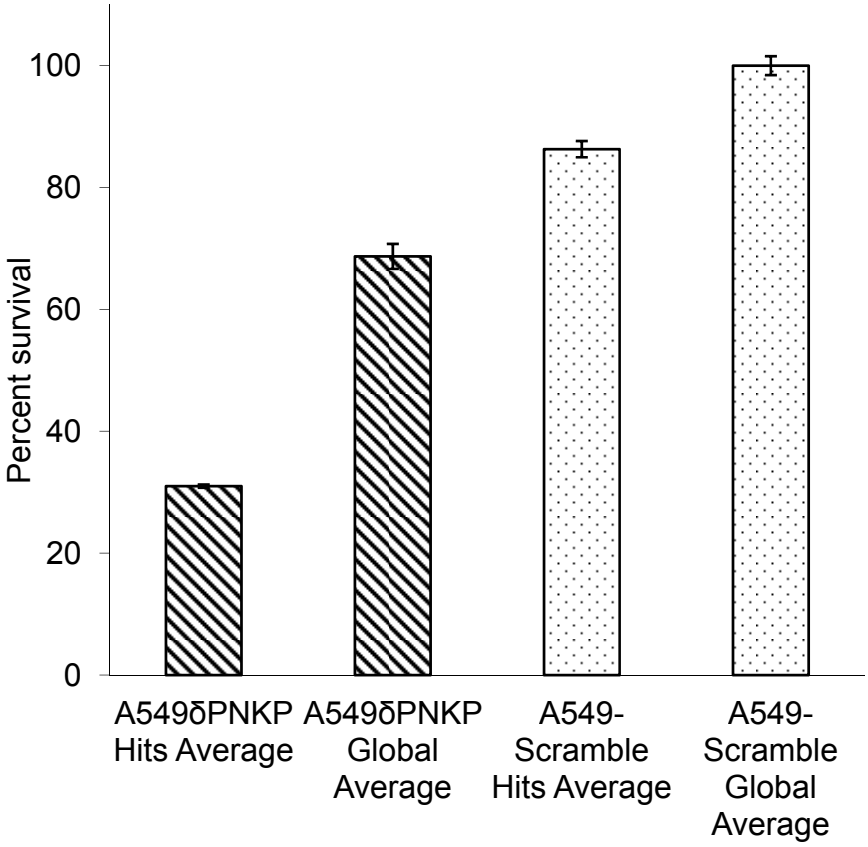

Figure 1

Author Manuscript Published OnlineFirst on September 7, 2012; DOI:10.1158/0008-5472.CAN-12-0939
Author manuscripts have been peer reviewed and accepted for publication but have not yet been edited.

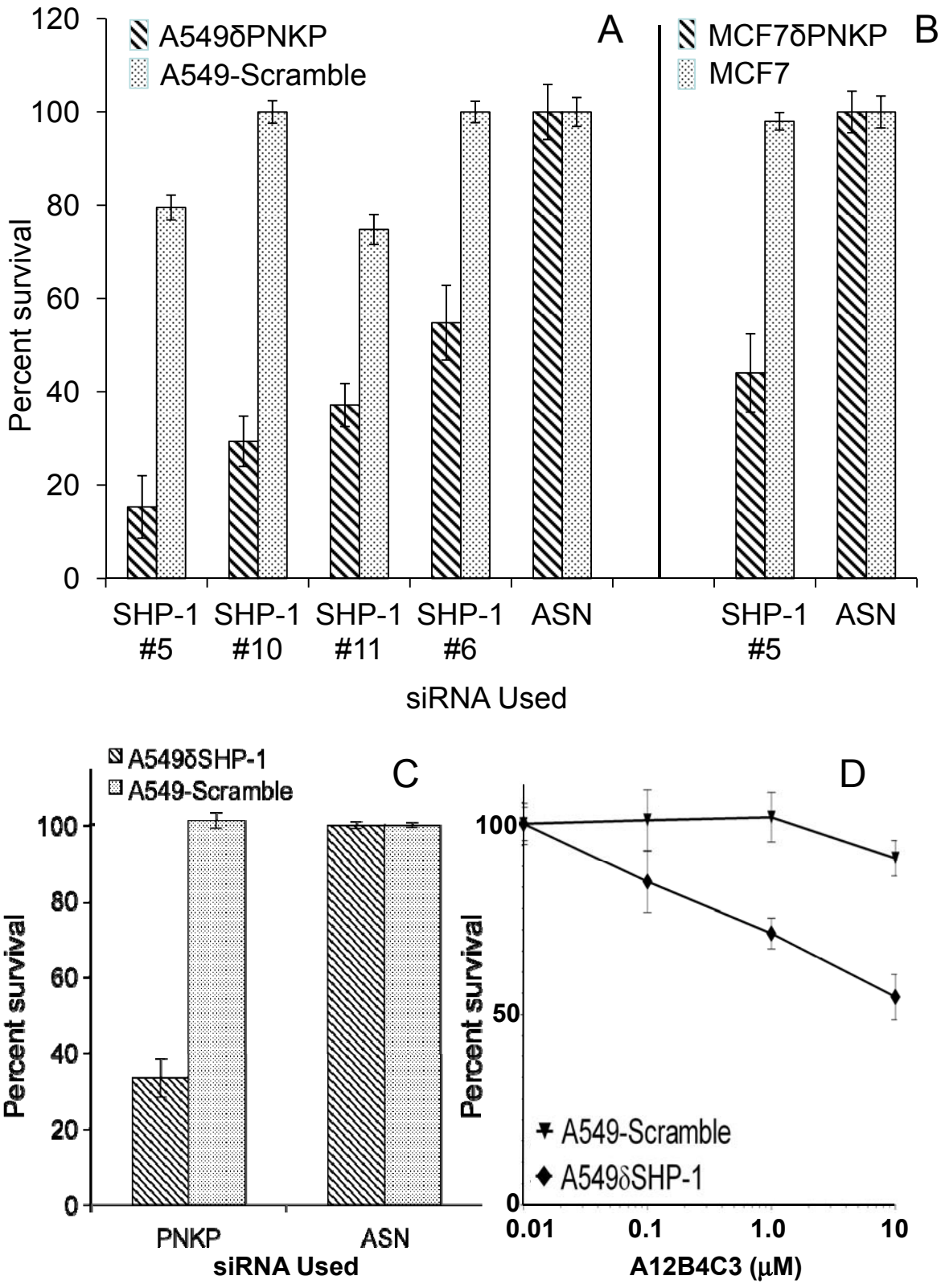

Figure 2

Author Manuscript Published OnlineFirst on September 7, 2012; DOI:10.1158/0008-5472.CAN-12-0939
Author manuscripts have been peer reviewed and accepted for publication but have not yet been edited.

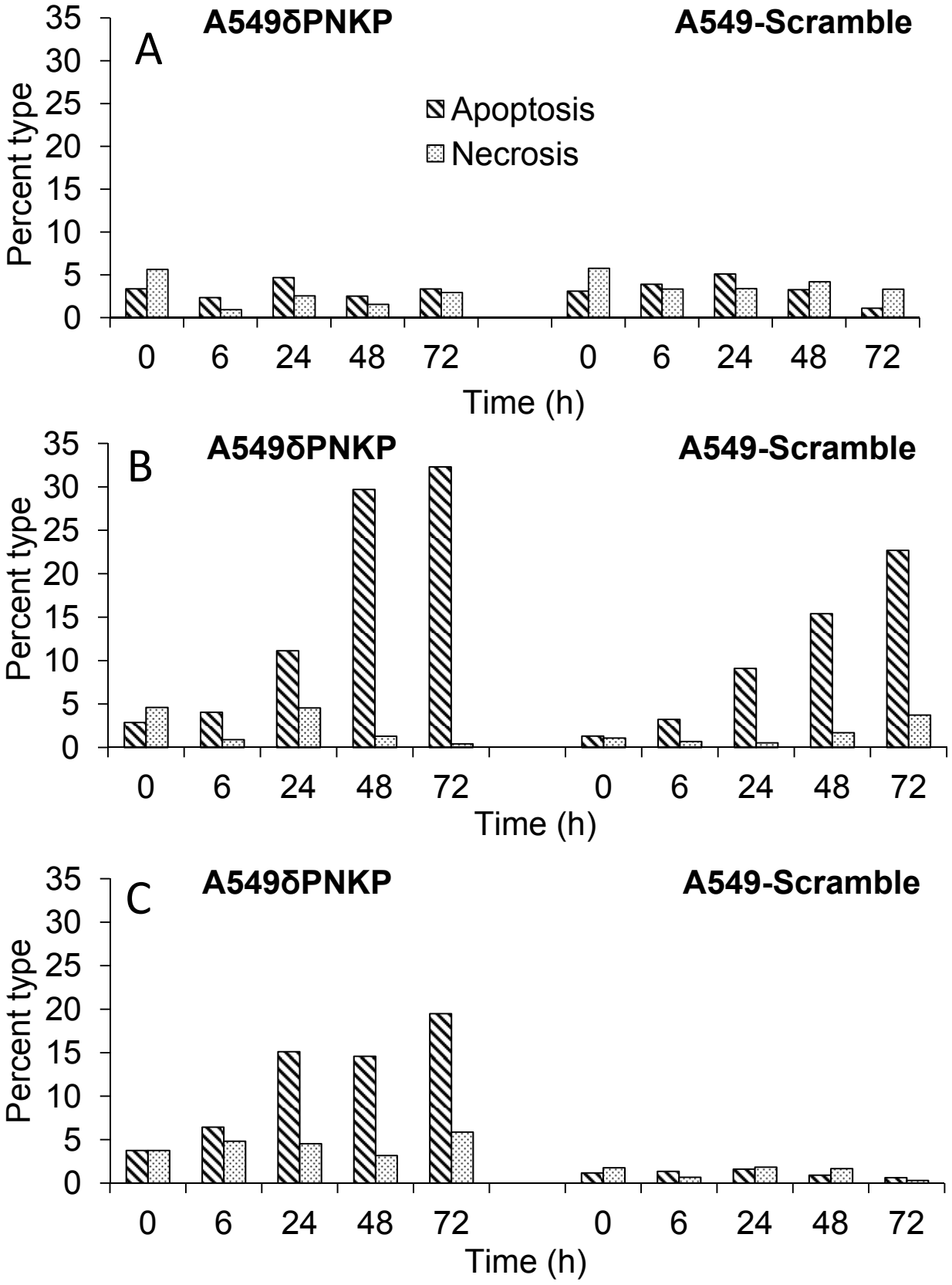

Figure 3

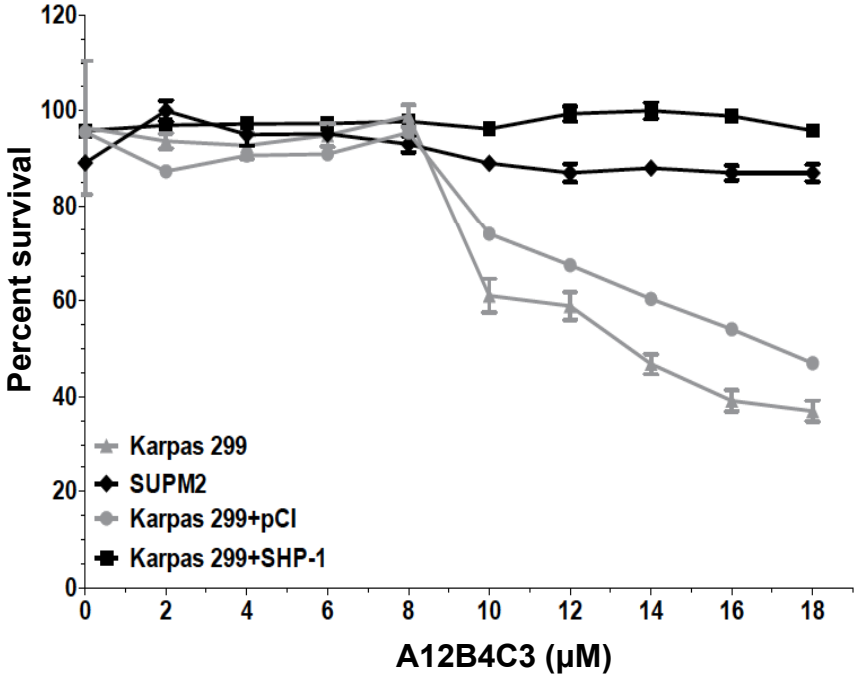

Figure 4

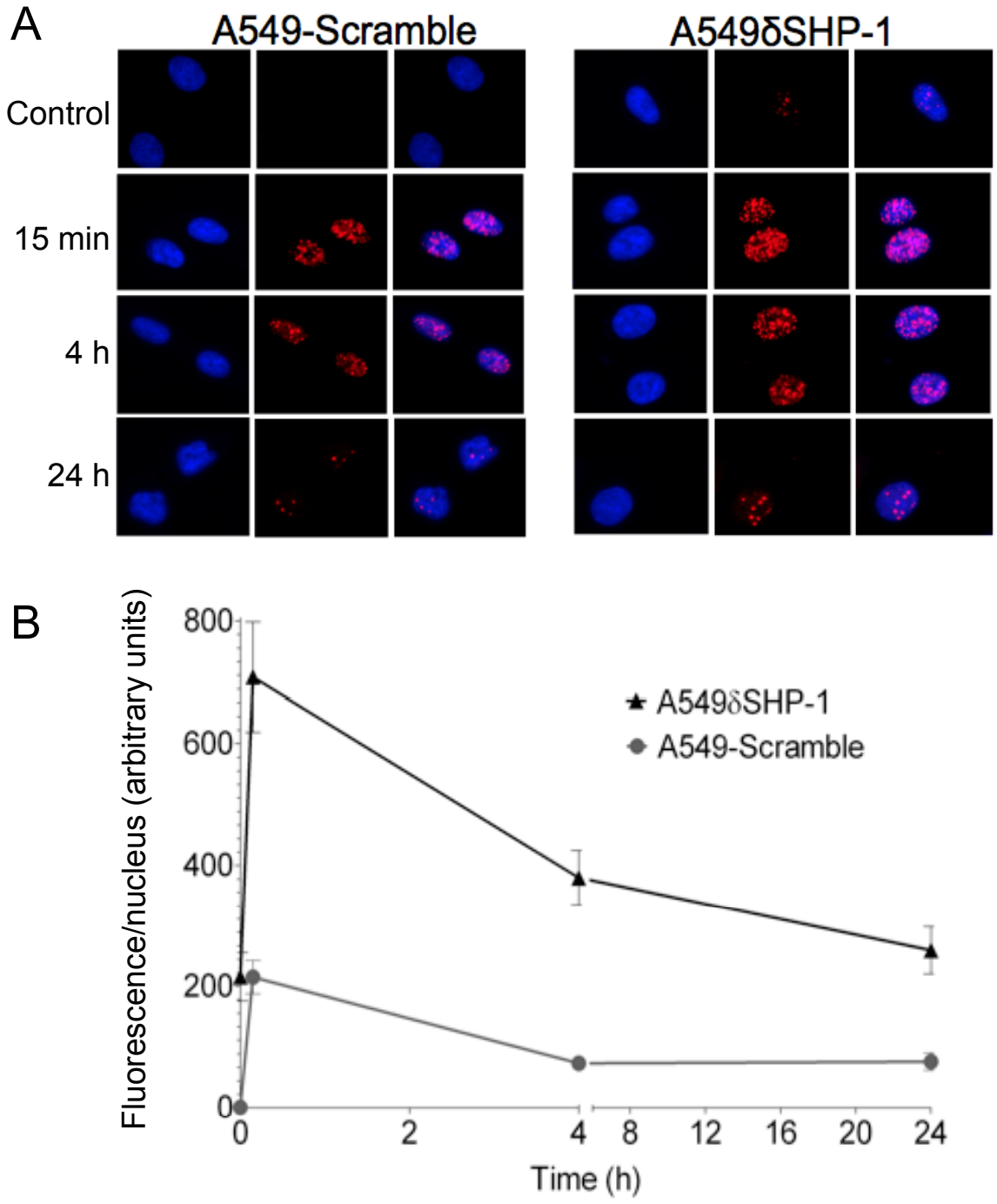

Figure 5

Author Manuscript Published OnlineFirst on September 7, 2012; DOI:10.1158/0008-5472.CAN-12-0939
Author manuscripts have been peer reviewed and accepted for publication but have not yet been edited.

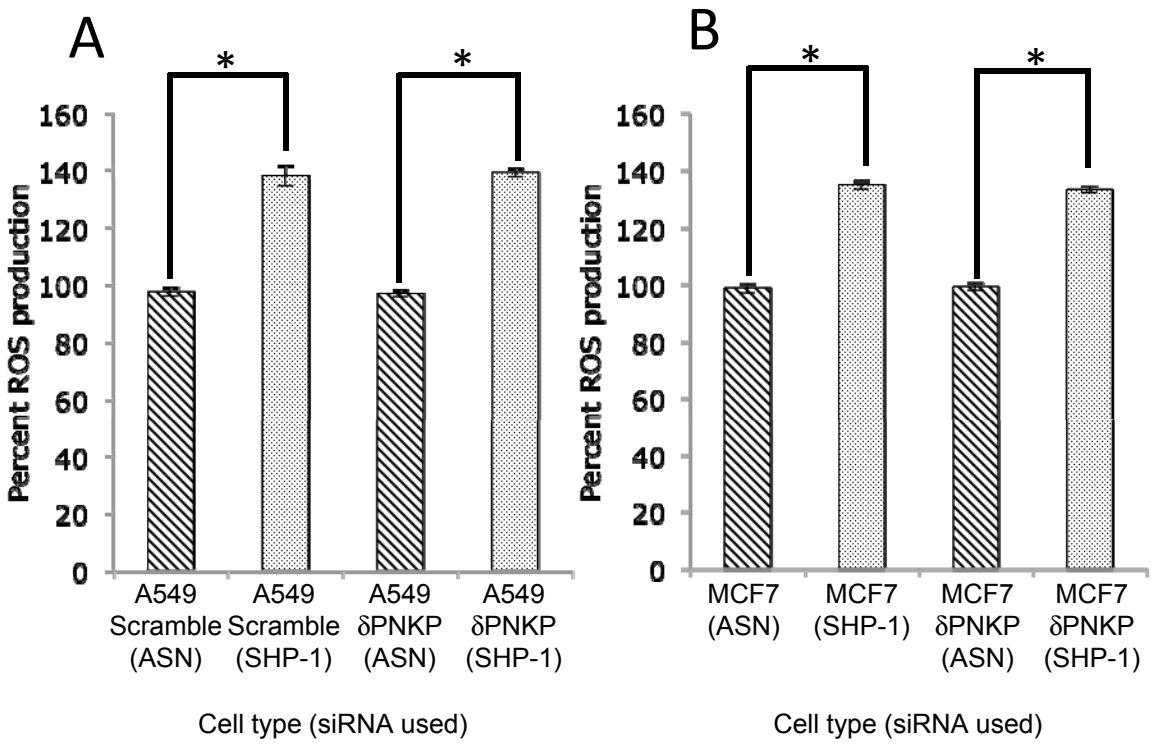

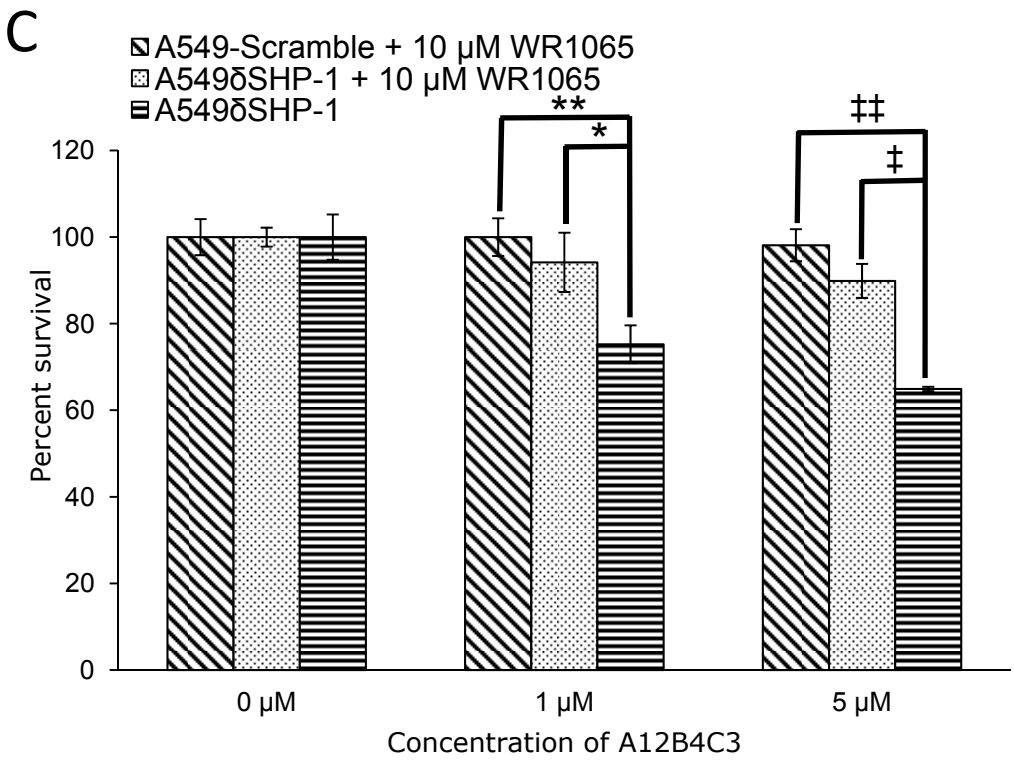

Figure 6

Author Manuscript Published OnlineFirst on September 7, 2012; DOI:10.1158/0008-5472.CAN-12-0939
Author manuscripts have been peer reviewed and accepted for publication but have not yet been edited.

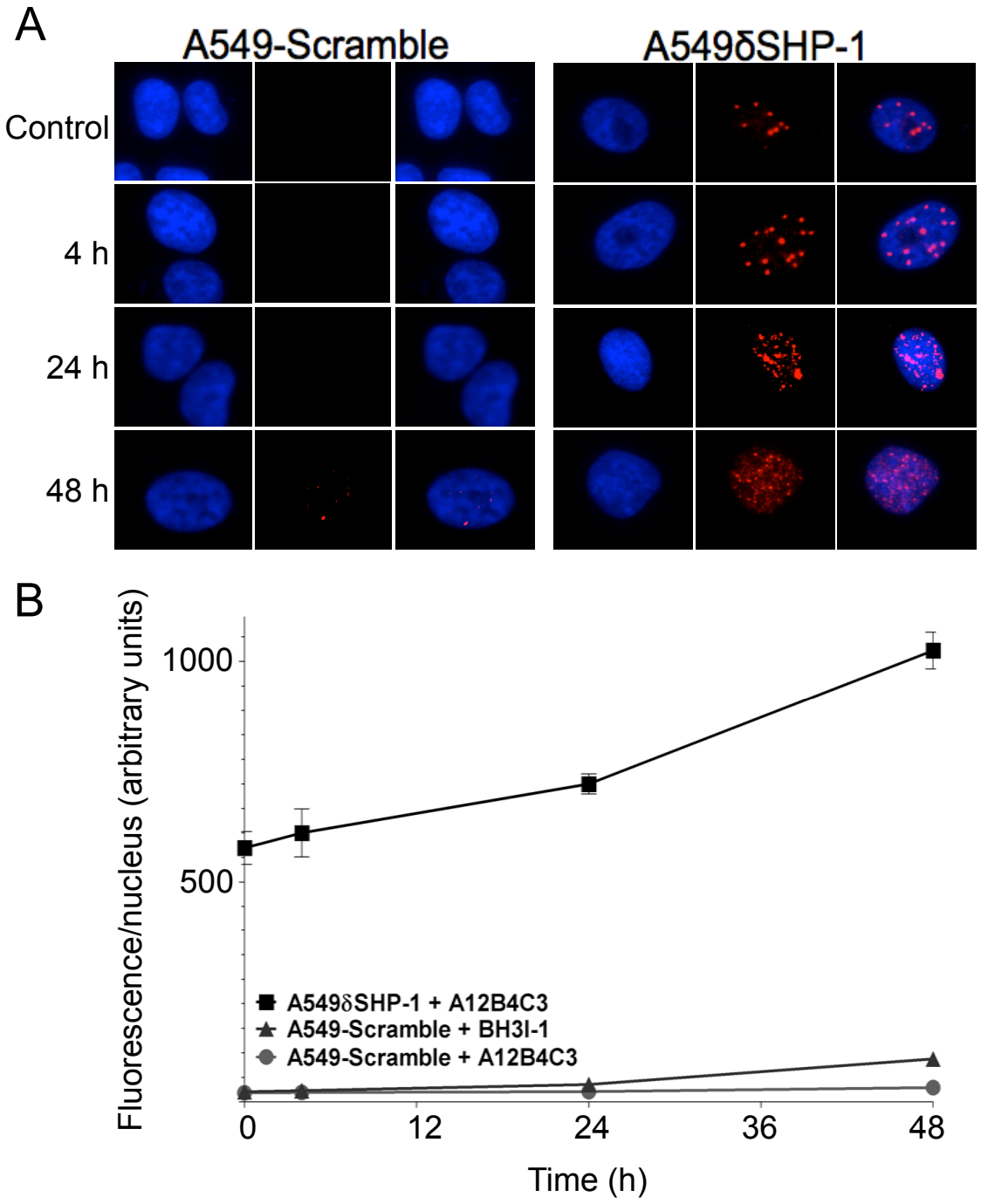

Figure 7